

Magnetoelastic Excitations in the Pyrochlore Spin Liquid $\text{Tb}_2\text{Ti}_2\text{O}_7$

T. Fennell,^{1,*} M. Kenzelmann,² B. Roessli,¹ H. Mutka,³ J. Ollivier,³ M. Ruminy,¹ U. Stuhr,¹ O. Zaharko,¹ L. Bovo,⁴
A. Cervellino,⁵ M. K. Haas,^{6,†} and R. J. Cava⁶

¹Laboratory for Neutron Scattering, Paul Scherrer Institut, 5232 Villigen PSI, Switzerland

²Laboratory for Developments and Methods, Paul Scherrer Institut, 5232 Villigen PSI, Switzerland

³Institut Laue Langevin, BP 156, 6, rue Jules Horowitz, 38042 Grenoble Cedex 9, France

⁴London Centre for Nanotechnology and Department of Physics and Astronomy, University College London,
17-19 Gordon Street, London WC1H 0AH, United Kingdom

⁵Swiss Light Source, Paul Scherrer Institut, 5232 Villigen PSI, Switzerland

⁶Department of Chemistry, Princeton University, Princeton, New Jersey 08540, USA

(Received 22 May 2013; published 8 January 2014)

At low temperatures, $\text{Tb}_2\text{Ti}_2\text{O}_7$ enters a spin liquid state, despite expectations of magnetic order and/or a structural distortion. Using neutron scattering, we have discovered that in this spin liquid state an excited crystal field level is coupled to a transverse acoustic phonon, forming a hybrid excitation. Magnetic and phononlike branches with identical dispersion relations can be identified, and the hybridization vanishes in the paramagnetic state. We suggest that $\text{Tb}_2\text{Ti}_2\text{O}_7$ is aptly named a “magnetoelastic spin liquid” and that the hybridization of the excitations suppresses both magnetic ordering and the structural distortion. The spin liquid phase of $\text{Tb}_2\text{Ti}_2\text{O}_7$ can now be regarded as a Coulomb phase with propagating bosonic spin excitations.

DOI: 10.1103/PhysRevLett.112.017203

PACS numbers: 75.10.Kt, 63.20.kd, 71.70.Ej, 78.70.Nx

Spin liquids [1] are often defined as correlated but fluctuating spin states with unbroken translation and spin rotation symmetry. In theory, many types of spin liquid can exist [2], but their experimental identification and classification is problematic. Since the absence of broken symmetry alone is not definitive and topological properties [2] are not experimentally accessible, one possibility is to study their excitations. These are often predicted to be exotic fractional quasiparticles such as spinons [3] or monopoles [4], but propagating bosonic excitations are possible in certain models [5–8].

$\text{Tb}_2\text{Ti}_2\text{O}_7$, which is often referred to as a spin liquid, does indeed remain in a magnetically disordered phase with spin dynamics down to 0.05 K [9]. The Tb^{3+} ions form a pyrochlore lattice and the spin interactions are antiferromagnetic ($\theta_{CW} = -19$ K), but the crystal field splits the 7F_6 free-ion term of Tb^{3+} to give a doublet ground state with Ising character. Classically, such a spin system should order, with $T_N \sim 1\text{--}2$ K predicted for $\text{Tb}_2\text{Ti}_2\text{O}_7$ [10,11]. Instead, the spin liquid state of $\text{Tb}_2\text{Ti}_2\text{O}_7$ develops below $T \sim 20$ K. At low temperature, pinch points appear in the diffuse neutron scattering, suggesting that this is a magnetic Coulomb phase governed by ice rules [12–15].

However, because Tb^{3+} is a non-Kramers ion, its degenerate electronic states are susceptible to Jahn-Teller distortions [16]. There is much experimental evidence of magnetoelastic effects below $T \sim 20$ K—Young’s modulus and elastic constants soften very significantly [17,18], structural Bragg peaks broaden anisotropically [19], there is a large dielectric anomaly [20], the low-temperature state is susceptible to pressure-induced magnetic order [21] and

magnetic field-induced structural modifications [22], acoustic phonons are strongly scattered by the spins [23]—but no distortion has been observed.

The strong expectations of long-range order and/or a structural distortion mean that the true nature of the spin liquid state and the mechanism of its existence are not evident. Usually, magnetoelastic coupling is a mechanism for the relief of frustration [24,25], but the spin liquid state in $\text{Tb}_2\text{Ti}_2\text{O}_7$ exists throughout the same temperature regime as the anomalous elastic properties, leading to the suggestion that both spin and structural degrees of freedom are frustrated in $\text{Tb}_2\text{Ti}_2\text{O}_7$ [26].

No theory simultaneously accounts for both the magnetoelastic phenomena and the spin liquid. Models based on single-ion magnetostriction mechanisms reproduce the bulk magnetoelastic properties [17,27] but make no account of the spin liquid; theories which focus on the evasion of long-range magnetic order by the introduction of quantum fluctuations by virtual crystal field excitations [28], hypothetical distortions [29,30], or anisotropic exchange [31] are successful in reproducing features of the diffuse neutron scattering [13,28,29,31], but have individual drawbacks (a magnetization plateau predicted in the case of virtual crystal field excitations [32] is strongly debated [33,34]; distortions [29,30] remain hypothetical, and single-ion singlet ground states [30] cannot account for the large elastic magnetic spectral weight [35]) and make no explanation of the magnetoelastic behavior.

We contend that the electronic and structural excitations of $\text{Tb}_2\text{Ti}_2\text{O}_7$ are mixed into hybrid fluctuations which we call magnetoelastic modes (MEMs), and this is at the origin

of the absence of magnetic order and structural distortion in $\text{Tb}_2\text{Ti}_2\text{O}_7$. We characterize a MEM, and demonstrate that it has both magnetic and phononic characters, which are visible at different wave vectors.

We used the same single crystal of $\text{Tb}_2\text{Ti}_2\text{O}_7$ as in Ref. [12]. It has no sign of any ordering transition between 0.35 and 50 K in its heat capacity, and by comparison with the series of $\text{Tb}_{2+x}\text{Ti}_{2-x}\text{O}_{7-x/2}$ powders reported in [26], its lattice parameter [$a = 10.155288(1)$ Å] suggests its stoichiometry is $\text{Tb}_{2.013 \pm 0.002}\text{Ti}_{1.987 \pm 0.002}\text{O}_{6.994 \pm 0.001}$. Further details of its characterization are to be found in the Supplemental Material [36]. Using the time-of-flight (TOF) spectrometer IN5 [37] at the Institut Laue Langevin, we surveyed a four-dimensional volume of $S(\mathbf{Q}, \omega)$. We measured at 0.05, 5, and 20 K using $\lambda_i = 4$ Å, and additionally at 0.05 K using $\lambda_i = 2$ and 7 Å. Using the triple-axis spectrometers (TAS) TASP (in combination with the neutron polarimetry device MuPAD) and EIGER at the SINQ, Paul Scherrer Institut, we investigated the polarization and temperature dependence of the MEM, respectively. In the polarized neutron scattering experiment, we measured non-spin-flip (NSF) and spin flip (SF) cross sections with the neutron polarization parallel to the scattering vector \mathbf{Q} , such that all magnetic scattering appears in the SF channel and nuclear scattering in the NSF channel. Data from the TAS experiments can be compared with cuts through the TOF spectra by scaling.

The known magnetic neutron scattering response of $\text{Tb}_2\text{Ti}_2\text{O}_7$ consists of elastic diffuse scattering [12,14,38], quasielastic scattering [13,39], and crystal field excitations (CFEs) [9]. Figures 1 and 2 show overviews of the inelastic scattering, with lower resolution extending to higher energy transfer and with higher energy resolution around the first CFE, respectively. We concentrate here on the MEM, which is a new feature. It is the weak but sharp mode extending out of the (2, 2, 0) position, between the two intense CFEs [Figs. 1(a)–1(d)]. A similar mode is visible at (1, 1, 1) [Fig. 1(e)], and the topmost part of the dispersion can be distinguished in nearby zones. Strong excitations are also visible at (0, 0, 8) [Fig. 1(f)], (3, 3, 7), and (5, 5, 5), but while those in low zones have their propagation vector (\mathbf{k}) parallel to the scattering vector (\mathbf{Q}), these have $\mathbf{k} \perp \mathbf{Q}$.

The first CFE is itself quite significantly dispersive at low temperatures. The interaction of the MEM with the first CFE, which is pulled up in energy where the two meet, can be seen in Fig. 2(a). There is no branch of the MEM reaching down to $\hbar\omega = 0$, below the CFE [Figs. 2(a)–2(c)]. Examination of the intensity throughout the isoenergy volume $S(\mathbf{Q}, \hbar\omega = 0.65 \text{ meV})$ shows no sharp features cut through it [Fig. 2(c)]. A broad, asymmetric peak is formed where the modes intersect, but, away from (2, 2, 0), two components can be distinguished in the CFE [Fig. 2(d)]. The MEM does not interact with the second CFE, as its dispersion passes just below it [Fig. 1(c)].

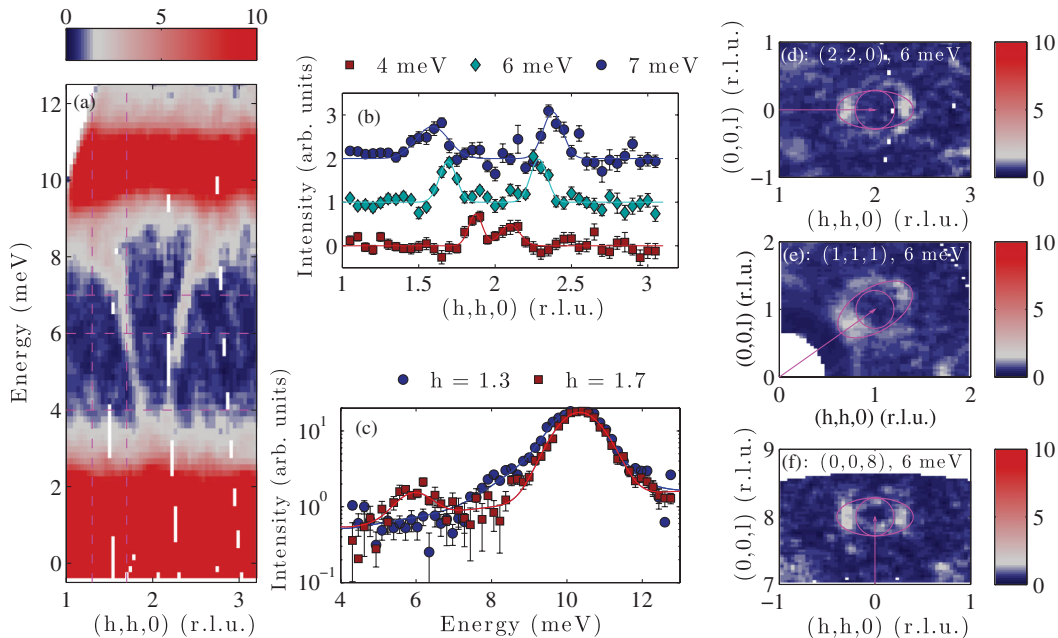


FIG. 1. Overview of the MEM. The sharp mode between the two intense crystal field excitations at 1.5 and 10 meV is the MEM (a). It is weak, but can be clearly identified in constant-energy cuts (b) (background levels offset by 1) and constant- \mathbf{Q} cuts (c) [cut positions are indicated in (a) by dashed lines]. Constant-energy maps show the MEM at (2, 2, 0) (d) and a similar mode at (1, 1, 1) (e). At these small wave vectors, the modes have their intensity parallel to the scattering vector (the arrow and ellipsoids show the scattering vector and highlight the intensity distribution, respectively). Excitations with similar dispersions are visible at large wave vectors [e.g., (0, 0, 8)] (f), but with a transverse intensity distribution.

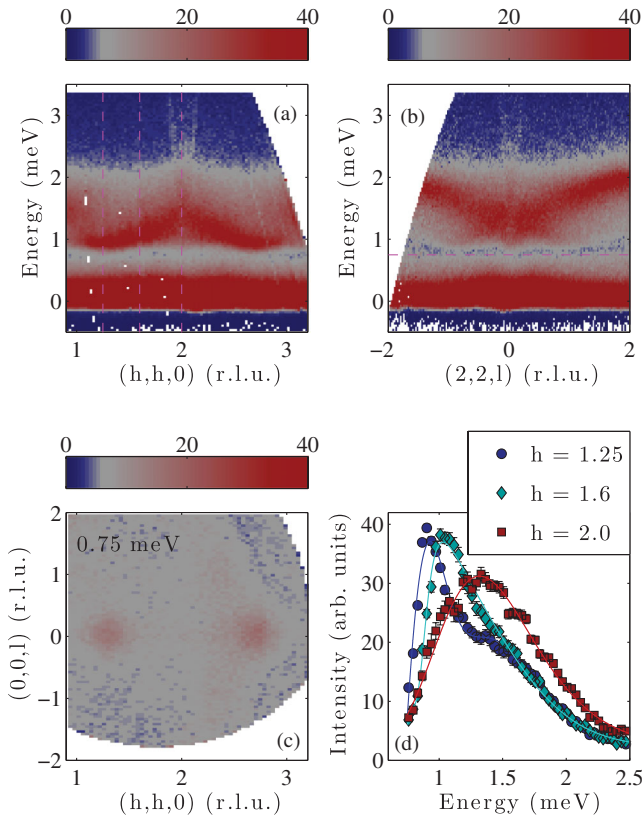


FIG. 2. Interaction of the MEM with the first crystal field excitation. At $(2, 2, 0)$, the MEM intersects with the first CFE (a) [this is the same view as Fig. 1(a), but with better energy resolution]. The MEM can be seen above the CFE. The MEM is faintly visible in the perpendicular direction (b), where some intensity concentrated around $(h, h, 0)$ is integrated in the cut. No sharp feature can be found extending below the CFE, as can also be seen in an intensity map at $E = 0.75$ meV [dashed line in (b)], i.e., in the gap (c). Constant- \mathbf{Q} cuts (d) [at positions indicated by dashed lines in (a)] show a two-component line shape for the CFE far away from $(2, 2, 0)$ and a single, broad, asymmetric, peak where the MEM meets the crystal field level.

MEMs can be observed at small wave vectors, typical of magnetic excitations. At $(2, 2, 0)$, we have determined explicitly that the MEM has a magnetic contribution by using polarized neutron scattering. As shown in Fig. 3(a), all of the scattering occurs in the spin flip channel, indicating that in fact there is no measurable nuclear contribution at this position. The intensity of the MEM is almost independent of energy until it approaches the second CFE where it may increase [Fig. 3(b)], in contrast to typical antiferromagnetic excitations which decrease in intensity with increasing energy.

Because magnetic neutron scattering is due to spin components perpendicular to \mathbf{Q} , and the wave vector \mathbf{k} of the mode is parallel to \mathbf{Q} , the MEM is a transverse mode (i.e., the spin fluctuations are perpendicular to its direction of propagation). In comparison, the excitations at large wave vectors are similar to transverse acoustic phonons—they

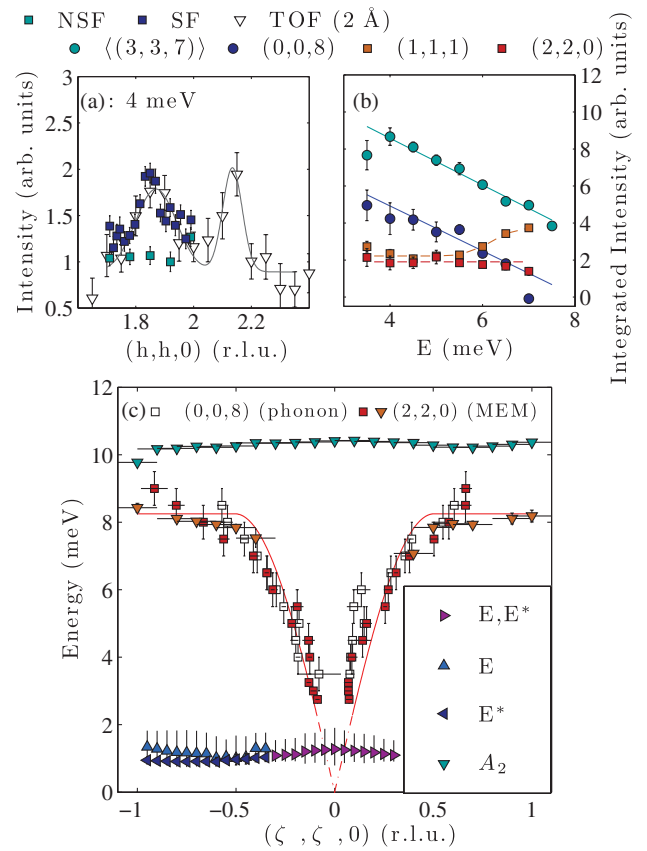


FIG. 3. Characterization of the excitations in $\text{Tb}_2\text{Ti}_2\text{O}_7$ at 0.05 K. Polarization analysis (a) shows that the scattering observed in the MEM at $(2, 2, 0)$ is magnetic. The integrated intensities (b) show that the modes at large wave vector have intensities which decrease with $\hbar\omega$, similar to phonons, while those at $(2, 2, 0)$ and $(1, 1, 1)$ have a different character. Fitted peak positions from constant-energy cuts (squares) and constant- \mathbf{Q} cuts (triangles) show that the dispersion of the magnetic mode is exactly the same as the phononlike mode (c). A_2 is the second CFE, E and E^* are the two components of the first CFE, where they can be distinguished. This level has been fitted with asymmetric Gaussian functions, and the bar indicates the half maximum height of the asymmetric line shapes. Elsewhere, the two bars indicate the error of the fitted peak position and the width of the integral used for the cut. Integrated intensities were extracted from energy slices such as Fig. 1(d) by summing all of the intensity above background within a ring fixed by the dispersion.

appear at large wave vectors (the phonon cross section depends on $|\mathbf{Q}|^2$), they are gapless (within the energy resolution of this setting of the spectrometer), their intensity decreases with $\hbar\omega$ [Fig. 3(b)], and they are intense when $\mathbf{k} \perp \mathbf{Q}$. However, if we compare the transverse magnetic mode at $(2, 2, 0)$ with the transverse phononlike mode $(0, 0, 8)$ [which is to say along $(h, h, 0)$ and $(h, h, 8)$, respectively], we see that the upper parts of their dispersions overlap precisely [Fig. 3(c)], suggesting they have a common origin, and that these are therefore mixed modes carrying both magnetic and structural fluctuations. We observe the magnetic part at small wave vectors, where the magnetic

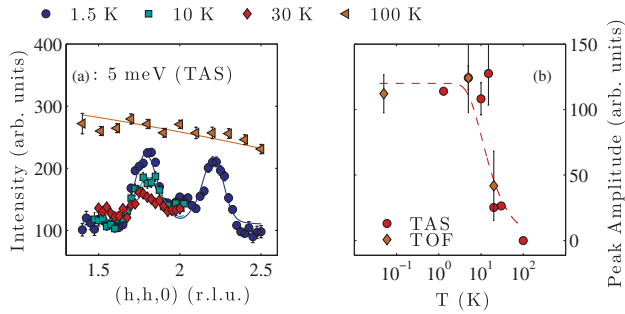


FIG. 4. Temperature dependence of the MEM. The MEM intensity collapses above 10 K (a). As the peak intensity falls above 10 K (b), a rising intensity which follows the magnetic form factor of Tb^{3+} (a) (100 K) also appears. This contribution originates from the thermal broadening of the nearby CFEs (it follows the Bose factor). The dashed line in (b) is $n_0 - n_1$ (scaled), where n_0 and n_1 are the thermal population factors of the ground and first excited states, respectively, of a two-level system with $\Delta = 1.4$ meV. TOF peak areas scaled to TAS peak amplitudes at 5 K.

form factor of Tb^{3+} is large, and the phononic part at large wave vectors, where the phonon cross section is large.

In Fig. 4, we show the temperature dependence of the MEM at $(2, 2, 0)$. Its intensity collapses in the range 10–20 K, again quite unlike a conventional phonon, which would become stronger at higher temperature. The detailed structure of interacting modes and two branches of the first CFE shown in Fig. 2 also collapses at $T \sim 20$ K. The CFE becomes a single level with (almost) none of the dispersion visible in Fig. 2(a).

The low-temperature dispersion of the first CFE indicates that the high-temperature single-ion excitations have been replaced by propagating excitons. The appearance of two branches in the exciton band indicates that, as in other rare earth pyrochlores, the exchange is anisotropic (different fluctuation directions become nondegenerate). The dispersion of these branches will provide a means to determine the anisotropic exchange parameters in $\text{Tb}_2\text{Ti}_2\text{O}_7$ [40].

In the usual crystal field scheme of $\text{Tb}_2\text{Ti}_2\text{O}_7$, the ground and first excited states (dominantly $a_4|\pm 4\rangle \pm a_5|\mp 5\rangle$ and $\pm b_5|\pm 5\rangle + b_4|\mp 4\rangle$, respectively) are connected not only by the operators J_{\pm} , but also J_x , J_y , and the quadrupole operators $O_{xz} = J_x J_z + J_z J_x = 1/2[(J_+ J_z + J_z J_+) + (J_- J_z + J_z J_-)]$ and $O_{yz} = J_y J_z + J_z J_y = 1/(2i)[(J_+ J_z + J_z J_+) - (J_- J_z + J_z J_-)]$. The finite matrix elements of J_x and J_y mean that the excitons are transverse fluctuations, and because of the quadrupole operators, they can mix with the transverse phonons [41]. The general features of such a coupling, which is linear in the relevant operators, are that its strength is largest at high energy but decreases as the energy difference between the modes increases; it vanishes as $(\mathbf{k}, \hbar\omega) \rightarrow 0$ and as the population of the CFE becomes comparable to that of the ground state [42]. This is in qualitative agreement with our observations—the MEM is undetectable at low energy (Fig. 2), while competition between the first two factors may result in the intensity distribution in the MEM shown in Fig. 3(b). The MEM vanishes in the relevant

temperature interval, as shown in Fig. 4. This temperature scale is also that in which the spin correlations evolve most strongly [12], suggesting that the magnetoelastic effects are not a coincidental property of the spin liquid phase.

The derivation of a Hamiltonian for $\text{Tb}_2\text{Ti}_2\text{O}_7$ remains challenging. The measurement of the excitation spectrum throughout a large volume of $S(\mathbf{Q}, \hbar\omega)$ shows no indication of global symmetry lowering or a soft mode associated with a structural transition. The key to the evasion of long-range magnetic order in $\text{Tb}_2\text{Ti}_2\text{O}_7$ seems to be the mixing of the first crystal field level with the ground state, which has been attempted theoretically in different ways [11,28,30,31,43], while the coupling of excitons and phonons we have observed suggests that both the quadrupole operators and anisotropic exchange are of central importance.

The low-temperature state of $\text{Tb}_2\text{Ti}_2\text{O}_7$ is ever more intriguing. In the spin sector we may hope for an emergent gauge theory, which must now contain power-law spin correlations [12] and a propagating bosonic excitation. Various theories of frustrated magnetism support dispersive excitations despite the absence of long-range magnetic order. In a quantum spin ice, the photon mode [6,7] looks superficially much like the MEM, and we speculate that the theory of a magnetoelastic spin liquid will ultimately resemble a quantum spin ice, with vibronic fluctuations replacing the quantum tunneling fluctuations. In this context, the microscopic meaning of our results is that exchange interactions and atomic wave functions depend on the position of atoms, which can themselves fluctuate in a correlated manner. Since an acoustic phonon is involved, passage of a hybrid fluctuation can reconfigure both spins and wave functions over a large distance. We suggest that $\text{Tb}_2\text{Ti}_2\text{O}_7$ should be viewed as an example of dynamical frustration [28,44] mediated by the spin-lattice coupling [26] evidenced here.

In conclusion, we have observed a magnetoelastic mode in the spin liquid phase of $\text{Tb}_2\text{Ti}_2\text{O}_7$. This mode is formed by the hybridization of the first excited crystal field level and the transverse acoustic phonons. The hybridization of the excitations disappears in the paramagnetic regime. We suggest that the coupling we have observed is at the origin of the anomalous magnetoelastic behavior of $\text{Tb}_2\text{Ti}_2\text{O}_7$. The existence of the magnetoelastic mode implies that the spin liquid phase of $\text{Tb}_2\text{Ti}_2\text{O}_7$ is a Coulomb phase supporting a propagating bosonic spin excitation.

We thank X. Thonon (ILL), M. Zolliker and M. Bartkowiak (PSI) for operation of dilution refrigerators; S. Fischer and W. Latscha for additional cryogenic support on EIGER; and A. Bullemer for assistance with cutting the sample. We are pleased to acknowledge discussions with O. Benton, A. T. Boothroyd, S. T. Bramwell, M. J. P. Gingras, A. Gukasov, H. Kadowaki, P. A. McClarty, C. Rugg, N. Shannon, and particularly J. Jensen. Neutron scattering experiments were carried out at the high flux reactor of the Institut Laue Langevin in Grenoble, France, and the continuous spallation neutron source SINQ at the Paul Scherrer Institut at Villigen PSI in

Switzerland, and work at PSI was partly funded by the Swiss National Science Foundation grant “Quantum Frustration in Model Magnets” (Grant No. 200021_140862).

Note added.—Recently, measurements of the quasielastic scattering have shown that it also contains a propagating mode [15]. The MEM at (1, 1, 1) is clearly visible in this study, but was interpreted as an acoustic phonon.

*Previous address: Institut Laue Langevin, BP 156, 6, rue Jules Horowitz, 38042, Grenoble Cedex 9, France.

tom.fennell@psi.ch

†Present address: Air Products and Chemicals Inc., Allentown, PA 18195, USA.

- [1] L. Balents, *Nature (London)* **464**, 199 (2010).
- [2] X.-G. Wen, *Phys. Rev. B* **65**, 165113 (2002).
- [3] T.-H. Han, J. S. Helton, S. Chu, D. G. Nocera, J. A. Rodriguez-Rivera, C. Broholm, and Y. S. Lee, *Nature (London)* **492**, 406 (2012).
- [4] C. Castelnovo, R. Moessner, and S. L. Sondhi, *Nature (London)* **451**, 42 (2008).
- [5] J. Robert, B. Canals, V. Simonet, and R. Ballou, *Phys. Rev. Lett.* **101**, 117207 (2008).
- [6] M. Hermele, M. P. A. Fisher, and L. Balents, *Phys. Rev. B* **69**, 064404 (2004).
- [7] O. Benton, O. Sikora, and N. Shannon, *Phys. Rev. B* **86**, 075154 (2012).
- [8] M. Levin and X.-G. Wen, *Rev. Mod. Phys.* **77**, 871 (2005).
- [9] J. S. Gardner, M. J. P. Gingras, and J. E. Greedan, *Rev. Mod. Phys.* **82**, 53 (2010).
- [10] B. C. den Hertog and M. J. P. Gingras, *Phys. Rev. Lett.* **84**, 3430 (2000).
- [11] Y. J. Kao, M. Enjalran, A. Del Maestro, H. R. Molavian, and M. J. P. Gingras, *Phys. Rev. B* **68**, 172407 (2003).
- [12] T. Fennell, M. Kenzelmann, B. Roessli, M. K. Haas, and R. J. Cava, *Phys. Rev. Lett.* **109**, 017201 (2012).
- [13] S. Petit, P. Bonville, J. Robert, C. Decorse, and I. Mirebeau, *Phys. Rev. B* **86**, 174403 (2012).
- [14] K. Fritsch, K. A. Ross, Y. Qiu, J. R. D. Copley, T. Guidi, R. I. Bewley, H. A. Dabkowska, and B. D. Gaulin, *Phys. Rev. B* **87**, 094410 (2013).
- [15] S. Guitteny, J. Robert, P. Bonville, J. Ollivier, C. Decorse, P. Steffens, M. Boehm, H. Mutka, I. Mirebeau, and S. Petit, *Phys. Rev. Lett.* **111**, 087201 (2013).
- [16] G. A. Gehring and K. A. Gehring, *Rep. Prog. Phys.* **38**, 1 (1975).
- [17] L. G. Mamsurova, K. S. Pigal’skii, and K. K. Pukhov, *JETP Lett.* **43**, 755 (1986); L. G. Mamsurova, K. S. Pigal’skii, K. K. Pukhov, N. G. Trusevich, and L. G. Shcherbakova, *J. Exp. Theor. Phys.* **67**, 550 (1988).
- [18] Y. Nakanishi, T. Kumagai, M. Yoshizawa, K. Matsuhira, S. Takagi, and Z. Hiroi, *Phys. Rev. B* **83**, 184434 (2011).
- [19] J. P. C. Ruff, B. D. Gaulin, J. P. Castellan, K. C. Rule, J. P. Clancy, J. Rodriguez, and H. A. Dabkowska, *Phys. Rev. Lett.* **99**, 237202 (2007).
- [20] L. G. Mamsurova, K. S. Pigal’skii, N. G. Trusevich, and L. G. Shcherbakova, *Sov. Phys. Solid State* **27**, 978 (1985).
- [21] I. Mirebeau, I. N. Goncharenko, P. Cadavez-Pares, S. T. Bramwell, M. J. P. Gingras, and J. S. Gardner, *Nature (London)* **420**, 54 (2002).
- [22] J. P. C. Ruff, Z. Islam, J. P. Clancy, K. A. Ross, H. Nojiri, Y. H. Matsuda, H. A. Dabkowska, A. D. Dabkowski, and B. D. Gaulin, *Phys. Rev. Lett.* **105**, 077203 (2010).
- [23] Q. J. Li, Z. Y. Zhao, C. Fan, F. B. Zhang, H. D. Zhou, X. Zhao, and X. F. Sun, *Phys. Rev. B* **87**, 214408 (2013).
- [24] O. Tchernyshyov, R. Moessner, and S. L. Sondhi, *Phys. Rev. Lett.* **88**, 067203 (2002).
- [25] G. W. Chern, C. J. Fennie, and O. Tchernyshyov, *Phys. Rev. B* **74**, 060405R (2006).
- [26] T. Taniguchi, H. Kadowaki, H. Takatsu, B. Fåk, J. Ollivier, T. Yamazaki, T. J. Sato, H. Yoshizawa, Y. Shimura, T. Sakakibara, T. Hong, K. Goto, L. R. Yaraskavitch, and J. B. Kycia, *Phys. Rev. B* **87**, 060408R (2013).
- [27] V. V. Klekovkina, A. R. Zakirov, B. Z. Malkin, and L. A. Kasatkina, *J. Phys. Conf. Ser.* **324**, 012036 (2011).
- [28] H. R. Molavian, M. J. P. Gingras, and B. Canals, *Phys. Rev. Lett.* **98**, 157204 (2007).
- [29] S. H. Curnoe, *Phys. Rev. B* **78**, 094418 (2008).
- [30] P. Bonville, I. Mirebeau, A. Gukasov, S. Petit, and J. Robert, *Phys. Rev. B* **84**, 184409 (2011).
- [31] S. H. Curnoe, *Phys. Rev. B* **88**, 014429 (2013).
- [32] H. R. Molavian and M. J. P. Gingras, *J. Phys. Condens. Matter* **21**, 172201 (2009).
- [33] S. Legl, C. Krey, S. R. Dunsiger, H. A. Dabkowska, J. A. Rodriguez, G. M. Luke, and C. Pfleiderer, *Phys. Rev. Lett.* **109**, 047201 (2012); P. J. Baker, M. J. Matthews, S. R. Giblin, P. Schiffer, C. Baines, and D. Prabhakaran, *Phys. Rev. B* **86**, 094424 (2012); E. Lhotel, C. Paulsen, P. Dalmas de Reotier, A. Yaouanc, C. Marin, and S. Vanishri, *Phys. Rev. B* **86**, 020410 (2012); L. Yin, J. S. Xia, Y. Takano, N. S. Sullivan, Q. J. Li, and X. F. Sun, *Phys. Rev. Lett.* **110**, 137201 (2013).
- [34] A. P. Sazonov, A. Gukasov, H. B. Cao, P. Bonville, E. Ressouche, C. Decorse, and I. Mirebeau, *Phys. Rev. B* **88**, 184428 (2013).
- [35] B. D. Gaulin, J. S. Gardner, P. A. McClarty, and M. J. P. Gingras, *Phys. Rev. B* **84**, 140402(R) (2011).
- [36] See Supplemental Material at <http://link.aps.org/supplemental/10.1103/PhysRevLett.112.017203> for further details of sample characterization.
- [37] J. Ollivier and J. M. Zanotti, *Collection SFN* **10**, 379 (2010).
- [38] J. S. Gardner, B. D. Gaulin, A. J. Berlinsky, P. Waldron, S. R. Dunsiger, N. P. Raju, and J. E. Greedan, *Phys. Rev. B* **64**, 224416 (2001).
- [39] Y. Yasui, M. Kanada, M. Ito, H. Harashina, M. Sato, H. Okumura, K. Kakurai, and H. Kadowaki, *J. Phys. Soc. Jpn.* **71**, 599 (2002).
- [40] J. G. Houmann, B. D. Rainford, J. Jensen, and A. R. Mackintosh, *Phys. Rev. B* **20**, 1105 (1979).
- [41] This argument is correct for fluctuations propagating along [111], the quantization direction of J_z for a single sublattice. Some departure from this description in terms of purely transverse fluctuations may be expected for the spins or fluctuations in other directions.
- [42] J. Jensen and A. R. Mackintosh, *Rare Earth Magnetism* (Clarendon Press, Oxford, England, 1991).
- [43] S. H. Curnoe, *Phys. Rev. B* **75**, 212404 (2007).
- [44] E. A. Goremychkin, R. Osborn, B. D. Rainford, R. T. Macaluso, D. T. Adroja, and M. M. Koza, *Nat. Phys.* **4**, 766 (2008).